



PII: S0017-9310(96)00191-3

A straightforward approximation to the equations governing convective flows in multi-component fluids

R. PÉREZ-CORDÓN and J. I. MENGUAL

Départamento de Física Aplicada I, Facultad de Ciencias Físicas, Universidad Complutense de Madrid, 28040-Madrid, Spain

(Received 22 June 1995 and in final form 16 May 1996)

Abstract—A straightforward non-linear extension of Boussinesq's approximation for two-component fluids is presented. The perturbative method proposed permits the numerical separation of the different orders in the obtained hierarchy of equations. The procedure is useful for the analysis of buoyancy driven flows and the stability of convective patterns. The fluid layer thicknesses, for which the Soret and Dufour effects must be retained in the equations, may be determined. The influence of the hydrostatic field on the heat equation may be obtained in relation to the layer thickness. The analysis permits us to obtain useful conclusions about the stability in two important examples of this kind of system: dry air and salt water. The method may be easily extended to multi-component fluids and to any other physical problem.

Copyright © 1996 Elsevier Science Ltd.

1. INTRODUCTION

As it is well known, the non-linear equations that describe the behavior of buoyancy driven flows (even in the simplest case of mono-component fluids) can be solved numerically, but not analytically. In the case of multi-component fluids, the number of equations is increased with the balances of the mixture components, and some new terms, such as those describing the Dufour and Soret effects, appear.

In the case of mono-component fluids, the equations have been simplified by Boussinesq [1], Spiegel and Veronis [2], Mihaljan [3], Malkus [4], Pérez-Cordón and Velarde [5, 6], Gray and Giorgini [7] and more recently, de Boer [8, 9].

Nowadays, some important phenomenological aspects of convection are being studied, such as: (i) the influence of temperature on thermal conductivity, viscosity and density [10, 11]; (ii) the increase in the number of hexagonal convection cells, induced by surface tension [12]; (iii) the spontaneous formation of spiral patterns in the Bénard-Rayleigh convection [13, 14]. The explanation of these phenomena require the introduction of non-linear terms into Boussinesq's equations. This requirement emphasizes the relevance of the quoted papers [5–6, 8–9].

In the case of multi-component fluids, some new phenomena such as diffusive flows, thermal diffusion, salt fingers, etc., are involved, and consequently a different analysis of the appropriate thermo-hydrodynamic equations is needed [11, 15]. The convective behavior of this kind of fluid has been considered in several papers [16, 17] by using linearized Boussinesq's equations. Nevertheless, in recent years,

considerable theoretical and experimental efforts have been made in order to clarify the influence of the different non-linear contributions on the appearance, development and stability of different convective structures in these fluids [18–23]. Consequently, a non-linear Boussinesq's approximation, valid for multi-component fluids, with all the non-linear contributions retained, is needed.

In this paper an approximation is presented, valid for two-component, Newtonian, non-reactive fluids (without any other restriction). The procedure may be easily extended to multi-component fluids. Special attention has been paid to the influence of the Dufour and Soret effects for different fluid layer thicknesses. The analysis is based on a three-parameter series expansion. In addition, the conditions that must be imposed on the fluid in order to get a numerical separation of the different orders in the hierarchy of equations obtained are analyzed. Finally, the crucial importance of correct choice of the scale units is pointed out.

2. FORMULATION OF THE PROBLEM

Let us consider a horizontal layer of a two-component non-reactive fluid, with thickness L and infinite surface. The convective movement is described by the following system of equations:

$$\frac{1}{\rho} \frac{d\rho}{dt} \equiv -\alpha \frac{dT}{dt} + \chi \frac{dP}{dt} + \gamma \frac{dc}{dt} = -\frac{dv_k}{dx_k} \quad (1)$$

$$\rho \frac{dc}{dt} = -\frac{dJ_k}{dx_k} \quad (2)$$

NOMENCLATURE

A_1	$\equiv \Delta \tilde{T} / \Delta T $ (non-dimensional monomial)	v_i	velocity vector
A_2	$\equiv \Delta \tilde{P} / \Delta P $ (non-dimensional monomial)	V	$\equiv \sqrt{gL \Delta\rho - \Delta\rho_A /\rho_0}$ (scale unit for velocity)
A_3	$\equiv \Delta \tilde{c} / \Delta c $ (non-dimensional monomial)	x_i	position vector.
B	thermal gradient	Greek symbols	
c	$\equiv c_1$ (mass-fraction of the first mixture component)	α	coefficient of thermal expansion
C_p	specific heat at constant pressure	α^*	$\equiv T_0 D_0^*/D_0$ (thermal diffusion factor)
C_v	specific heat at constant volume	β	non-dimensional gradient of temperature
D	molecular diffusion coefficient	β_p	non-dimensional gradient of pressure
D^*	thermal diffusion (Soret) coefficient	β_c	non-dimensional gradient of concentration
D^{**}	Dufour coefficient	γ	$\equiv 1/\rho \partial\rho/\partial c$
g	gravitational acceleration	δ_{ij}	Kronecker's delta
Gr	$\equiv \alpha_0/\chi_0 C_p \rho_0$ (Grüneisen's constant)	Δ	denotes difference taken between the upper and the lower surface of the fluid layer
h_1, h_2	partial specific enthalpies of the first and second mixture components	ε_1	$\equiv \alpha_0 \Delta T $ (non-dimensional parameters)
J_i^0	heat flow vector	ε_2	$\equiv \chi_0 \rho_0 g L$ (non-dimensional parameters)
J_i^*	reduced heat flow vector	ε_3	$\equiv \gamma_0 \Delta c $ (non-dimensional parameters)
K	thermal conductivity	η_1, η_2	shear and bulk viscosity coefficients
L	fluid layer thickness	κ	$\equiv K/C_p \rho_0$ (thermal diffusivity)
Le	$\equiv D_0/\kappa_0$ (Lewis number)	μ_1	chemical potential of the first mixture component
MT_i, Mp_i, Mc_i	molecular diffusion flow vector contributions	$\mu_{1,1}^c$	$\equiv \partial\mu_1/\partial c$
P	pressure	ν	$\equiv \nu_1/\rho_0$ (kinematic viscosity)
Pr	$\equiv \nu_0/\kappa_0$ (Prandtl number)	ρ	density
QT_i, QP_i, Qc_i	heat flow vector contributions	τ_{ij}	viscous stress tensor
R	$\equiv \sqrt{gL^3 \alpha_0 (\Delta T_A - \Delta T)/(\nu_0 \kappa_0)}$ (Rayleigh number)	χ	isothermal compressibility.
R_{eff}	$R - R_s$ (effective Rayleigh number)	Subscripts and superscripts	
R_s	$\equiv \sqrt{gL^3 \gamma_0 (-\Delta c/\nu_0 D_0)}$ (solute Rayleigh number)	0	denotes reference state
s	specific entropy	s	denotes reference hydrostatic field
Sc	$\equiv \nu_0/D_0$ (Schmidt number)	A	denotes 'hydrostatic adiabatic field'
S_p	$\equiv \gamma_0^2 (1 - c_0)/\rho_0 \mu_{1,1}^c \chi_0$ (baro-diffusivity separation number)	\sim	denotes perturbation
S_T	$\equiv c_0 (1 - c_0) D_0^* \gamma_0 / D_0 \alpha_0$ (Soret separation number)	'	denotes non-dimensional quantity.
t	time		
T	temperature		

$$\rho \frac{dv_i}{dt} = -\frac{\partial P}{\partial x} + \frac{\partial \tau_{ii}}{\partial x_j} - g\rho\delta_{i3} \quad (3) \quad -J_k = \rho \left(c(1-c)D^* \frac{\partial T}{\partial x_k} + D \left(\frac{\partial c}{\partial x_k} - \frac{\gamma(1-c)}{\rho\mu_{1,1}^c} \frac{\partial P}{\partial x_k} \right) \right)$$

$$\rho C_p \frac{dT}{dt} - \alpha T \frac{dP}{dt} = -\frac{\partial J_k^*}{\partial x_k} - J_k \frac{\partial (h_1 - h_2)}{\partial x_k} + \tau_{ij} \frac{\partial v_i}{\partial x_j} \quad (k = 1, 2, 3) \quad (6)$$

$$-J_{qi}^* = K \frac{\partial T}{\partial x_i} + \rho c \mu_{1,1}^c T D^{**} \left(\frac{\partial c}{\partial x_i} - \frac{\gamma(1-c)}{\rho\mu_{1,1}^c} \frac{\partial P}{\partial x_i} \right) \quad (4)$$

where

$$\tau_{ij} = \frac{\eta_2}{3} \frac{\partial v_k}{\partial x_k} \delta_{ij} + \eta_1 \left(\frac{\partial v_j}{\partial x_i} + \frac{\partial v_i}{\partial x_j} - \frac{2}{3} \frac{\partial v_k}{\partial x_k} \delta_{ij} \right) \quad (5) \quad \text{The symbols appearing in the previous equations are defined on the nomenclature pages. Einstein's con-}$$

$$(i = 1, 2, 3). \quad (7)$$

vection about addition over repeated indexes has been used. The barycentric substantial time derivative has been employed :

$$\frac{d}{dt} \equiv \frac{\partial}{\partial t} + v_k \cdot \frac{\partial}{\partial x_k} \quad (k = 1, 2, 3). \quad (8)$$

The fluid material properties : ρ , C_p , μ_1 , η_1 , η_2 , K , D , D^* , D^{**} , α , χ and γ are assumed to be functions of temperature T , pressure P , and mass fraction of the component $1 - c_1$, of the fluid. These functions can be expanded in Taylor series with respect to variables T , P and c_1 . The reference values T_0 , P_0 and c_0 correspond to the lower non-perturbed boundary of the layer. This procedure permits the evaluation of the non-linear terms and their distribution in the different orders into the obtained hierarchy of equations.

In what follows, the critical hydrostatic fields from which the onset of convection takes place, will be described.

3. CRITICAL HYDROSTATIC FIELDS

As it is well known, a fluid layer stays at rest, for small perturbations as long as the critical effective Rayleigh number is not reached [16]. The stationary state established in the layer at rest is called the 'hydrostatic field' (H.F.). A two-component H.F. is described by the following system of equations :

$$\frac{dJ_{3s}}{dx_3} = 0 \quad (9)$$

$$\frac{dJ_{3s}^Q}{dx_3} = \frac{d}{dx_3} (J_{3s}^* + J_{3s}(h_1 - h_2)) \quad (10)$$

$$\frac{dP}{dx_3} = -\rho g \quad (11)$$

where x_3 is the spatial coordinate perpendicular to the layer surface. The subscript s will be used in reference to H.F. in this paper. At present, our main aim is to separate the contributions of the H.F. and of the perturbations in equations (1)–(4).

From Jeffreys' work [24], the adiabatic hydrostatic field (A.H.F.) is used instead of the critical H.F., for mono-component fluids. As it is well known, the buoyancy forces give rise to the ascent of fluid portions from the bottom to the top of the layer. This process may be considered an adiabatic expansion. In addition, for multi-component fluids, there are no material fluxes because the diffusive relaxation time is greater than the thermal relaxation time. In the case of non-reactive fluids, the adiabatic temperature variations take place at constant chemical composition. Consequently, for a fluid layer of this kind at rest, an A.H.F. is characterized by the conditions $J_q = 0$ and $J_1 = 0$. In our case (non-reactive multi-component fluid, in a gravitational field), these conditions are equivalent to $ds/dx_3 = 0$ and $dc/dx_3 = 0$.

In general, the A.H.F. lacks physical reality because of the incompatibility of the equations describing the

hydrostatic fields with the condition, $ds/dx_3 = 0$. This incompatibility is even more drastic if the condition $dc/dx_3 = 0$ is also imposed. This condition is necessary in order to get a fluid layer with a homogeneous composition, through which the so-called adiabatic temperature gradient exists. An example of such a fluid is often used to analyze the Earth's atmosphere stability [25, 26]. In fact, the homogeneity in the composition of atmospheric or ocean-water layers is an obvious consequence of convective movements. In the stationary state, a layer of these characteristics is destabilized by thermal-diffusion and barodiffusion, among other causes. The differences existing between the H.F. and the hypothetical A.H.F. are appreciable. As an example, Table 1 show some comparative data for : a gas mixture N_2/O_2 , 76% wt and a NaCl aqueous solution, 6% wt. The first case may be considered similar to dry air and the second to ocean-water. In both cases the results refer to fluid layers sealed with impervious and conductive boundaries. The H.F. will be used in order to get a numerically consistent series expansion of the perturbation equations (1)–(4).

In the next section the perturbation equations will be obtained.

4. PERTURBATION EQUATIONS

In what follows, the superscript \sim will be used with reference to the perturbations from the H.F. Consequently, the temperature, pressure and concentration may be written by splitting the contributions of the H.F. and the perturbations as follows :

$$T \equiv T_s + \tilde{T} \quad P \equiv P_s + \tilde{P} \quad \text{and} \quad c \equiv c_s + \tilde{c}.$$

The introduction of these expressions into equations (1)–(4) and the subtraction of the relationships (9)–(11) from equations (2)–(4), respectively, lead to the following perturbation equations :

$$-\alpha \left(\frac{d\tilde{T}}{dt} + v_3 \cdot \frac{dT_s}{dx_3} \right) + \chi \left(\frac{d\tilde{P}}{dt} + v_3 \cdot \frac{dP_s}{dx_3} \right) + \gamma \left(\frac{d\tilde{c}}{dt} + v_3 \cdot \frac{dc_s}{dx_3} \right) = -\frac{\partial v_k}{\partial x_k} \quad (12)$$

$$\rho \left(\frac{d\tilde{c}}{dt} + v_3 \cdot \frac{dc_s}{dx_3} \right) = -\frac{\partial (J_i - \delta_{i3} J_{3s})}{\partial x_i} \quad (13)$$

$$\rho \frac{dv_i}{dt} = \frac{\partial \tilde{P}}{\partial x_i} + \frac{\partial \tau_{ij}}{\partial x_j} - g(\rho - \rho_s) \delta_{i3} \quad (14)$$

$$\begin{aligned} \rho C_p \left(\frac{d\tilde{T}}{dt} + v_3 \cdot \frac{dT_s}{dx_3} \right) - \alpha (\tilde{T} + T_s) \times \left(\frac{d\tilde{P}}{dt} + v_3 \cdot \frac{dP_s}{dx_3} \right) \\ = \frac{\partial^* (J_i - \delta_{i3} J_{3s})}{\partial x_i} - J_i \frac{\partial (h_1 - h_2)}{\partial x} + J_{3s} \frac{\partial (h_{1s} - h_{2s})}{\partial x} \\ + \tau_{ij} \frac{\partial v_i}{\partial x_j}. \end{aligned} \quad (15)$$

Table 1. Estimated data for differences between top and bottom boundaries of several layers ($T_0 = 300$ K, $P_0 = 10^5$ Pa, $J_{3s} = 0$ and $R_{\text{eff}} = 657.5$)

L [m]	ΔP_s [Pa]	ΔT [K]	ΔT_A [K]	$\Delta T_s - \Delta T_A$ [K]	Δc
<i>N₂/O₂ mixtures (Dry air), $c_0 = 0, 76$ (N₂)</i>					
10^{-3}	10^{-2}	-6×10^3	-10^{-5}	-6×10^3	-7×10^{-2}
10^{-2}	10^{-1}	-6	-10^{-4}	-6	-7×10^{-5}
10^{-1}	1	-7×10^{-3}	-10^{-3}	-6×10^{-3}	$+2 \times 10^{-7}$
1	10	-10^{-2}	-10^{-2}	-10^{-4}	$+2 \times 10^{-6}$
10	10^2	-10^{-1}	-10^{-1}	-10^{-3}	$+2 \times 10^{-5}$
10^2	10^3	-1	-1	-10^{-2}	$+2 \times 10^{-4}$
10^3	10^4	-10	-10	-10^{-1}	$+2 \times 10^{-3}$
<i>NaCl aqueous solutions (salt water), $c_0 = 0.94$ (H₂O)</i>					
10^{-3}	10	-1	-10^{-7}	-1	-1×10^{-4}
10^{-2}	10^2	-1×10^{-3}	-10^{-6}	-1×10^{-3}	-1×10^{-7}
10^{-1}	10^3	-5×10^{-3}	-10^{-5}	-5×10^{-3}	$+2 \times 10^{-8}$
1	10^4	-5×10^{-2}	-10^{-4}	-5×10^{-2}	$+2 \times 10^{-7}$
10	10^5	-5×10^{-1}	-10^{-3}	-5×10^{-1}	$+2 \times 10^{-6}$
10^2	10^6	-5	-10^{-2}	-5	$+2 \times 10^{-5}$
10^3	10^7	-5×10	-10^{-1}	-5×10	$+2 \times 10^{-4}$

In the next section these equations will be non-dimensionalized.

5. NON-DIMENSIONALIZATION OF THE EQUATIONS

In order to obtain the non-dimensionalization of the equations, it is necessary to choose adequately the corresponding scale units. Unfortunately, the magnitude orders of the scale units for the H.F. and for the perturbations are different in most cases. In the following, we will state the different scale units that will be used throughout the paper:

(1) L , for length; L/V , for time and the corresponding values in the reference state ($\rho_0, \alpha_0, \chi_0, \gamma_0, \eta_{10}, \eta_{20}, \mu_{1,10}^c, C_{p0}, C_{v0}, D_0, D_0^*, D_0^{**}, K_0, h_{10}$ and h_{20}) for the fluid properties. We will also use the definition $\Omega \equiv \eta_2/\eta_1$.

(2) In the case of the H.F., the scale units are the differences (in absolute value) between boundaries of the non-perturbed fluid layer: $|\Delta T|$ for T , $|\Delta P| \equiv \rho_0 g L$ for P and $|\Delta c|$ for c_i . In the case of the perturbed magnitudes, absolute maximum values, $|\Delta \tilde{T}|$, $|\Delta \tilde{P}| \equiv \rho_0 V^2$ and $|\Delta \tilde{c}|$ will be used.

(3) A realistic scale unit for the magnitude velocity, V , is the 'free ascent' velocity, corrected by the effect that the adiabatic ascent produces on the flotation forces: $V = \sqrt{gL(\Delta\rho - \Delta\rho_A/\rho_0)}$, where $\Delta\rho$ is the density difference between the boundaries of the layer and $\Delta\rho_A$ is the difference between the boundaries of an A.H.F. in the layer.

(4) For the sake of convenience, the following relationships will be used:

$$A_1 \equiv \frac{|\Delta \tilde{T}|}{|\Delta T|}$$

$$A_2 \equiv \frac{|\Delta \tilde{P}|}{|\Delta P|} \simeq \frac{V^2}{gL} \equiv (\alpha_0(\Delta T_A - \Delta T) + \gamma_0 \Delta c) \ll 1$$

$$A_3 \equiv \frac{|\Delta \tilde{c}|}{|\Delta c|}$$

ΔT_A is the temperature difference between boundaries corresponding to the so-called 'adiabatic gradient'.

In the case of gases, the difference between the adiabatic temperature gradient and the hydrostatic gradient, from which the layer becomes unstable, may be large ($|\Delta T| \simeq |\Delta \tilde{T}| \gg |\Delta T_A|$) for thin layers, or small ($|\Delta T| \simeq |\Delta T_A| \gg |\Delta \tilde{T}|$) for thick layers, see Table 1. Equations (12)–(15) may be rewritten by using all the above quoted scale units:

$$-\alpha \frac{d(T'_s + A_1 \tilde{T}')}{dt'} \varepsilon_1 + \chi \frac{d(P'_s + A_2 \tilde{P}')}{dt'} \varepsilon_2 + \gamma \frac{d(c'_s + A_3 \tilde{c}')}{dt'} \varepsilon_3 = -\frac{\partial v'_k}{\partial x'_k} \quad (16)$$

$$\left(\sqrt{\frac{Sc}{Le}} (R - Le R_s) \right) \rho \frac{d(c'_s + A_3 \tilde{c}')}{dt'} = \left(S_\tau \frac{\varepsilon_1}{\varepsilon_2} \right) \frac{\partial (MT_i - MT_{3s} \delta_{is})}{\partial x'_i} + \frac{\partial (Mc_i - Mc_{3s} \delta_{3i})}{\partial x'_i} - \left(S_p \frac{\varepsilon_2}{\varepsilon_3} \right) \frac{\partial (MP_i - MP_{3s} \delta_{3i})}{\partial x'_i} \quad (17)$$

$$\rho \frac{dv'_i}{dt'} = -\frac{\partial \tilde{P}'}{\partial x'_i} + \sqrt{\frac{Pr}{R - Le R_s}} \left(\frac{\partial \tau'_{ji}}{\partial x'_i} \right) - \frac{\rho' - \rho'_s}{A_3} \delta_{i3} \quad (18)$$

$$\sqrt{Pr(R - Le R_s)} \left(\rho' c'_p \frac{d(T'_s + A_1 \tilde{T}')}{dt'} - \left(1 - \frac{c_{p0}}{C_{v0}} \right) \frac{\varepsilon_2}{\varepsilon_1} \alpha \times \left(1 + \frac{\varepsilon_1}{\alpha_0 T_0} (T'_s + A_1 \tilde{T}') \right) \times \frac{d(P'_s + A_2 \tilde{P}')}{dt'} \right)$$

$$\begin{aligned}
&= \frac{\partial(QT_i - QT_{3s}\delta_{3i})}{\partial x'_i} + \left(1 - \frac{C_{v0}}{C_{p0}}\right) \left(\frac{S_T Le \varepsilon_3}{S_p \varepsilon_1}\right) \\
&\quad \times \frac{\partial(Qc_i - Qc_{3s}\delta_{3i})}{\partial x'_i} - \frac{S_T Le \varepsilon_2}{\varepsilon_i} \frac{\partial(QP_i - QP_{3s}\delta_{3i})}{\partial x'_i} \\
&\quad + \frac{S_T Le \alpha_0 |\Delta(h_1 - h_2)|}{\gamma_0 C_{p0}} \left(MT_k \frac{\partial(h_1 - h_2)}{\partial x_k} \right. \\
&\quad \left. - MT_{3s} \frac{\partial(h_1 - h_2)_s}{\partial x_3} \right) + \frac{Le \alpha_0 |\Delta(h_1 - h_2)| \varepsilon_3}{\gamma_0 C_{p0} \varepsilon_1} \\
&\quad \times \left(Mc_k \frac{\partial(h_1 - h_2)}{\partial x_k} - Mc_3 \frac{\partial(h_1 - h_2)}{\partial x_3} \right) \\
&\quad - \frac{S_p Le \alpha_0 |\Delta(h_1 - h_2)| \varepsilon_2}{\gamma_0 C_{p0} \varepsilon_1} \left(MP_k \frac{\partial(h_1 - h_2)}{\partial x_k} \right. \\
&\quad \left. - MP_{3s} \frac{\partial(h_1 - h_2)_s}{\partial x_3} \right) + \frac{Pr Gr A_2 \varepsilon_2}{\varepsilon_1} \tau_{ij} \frac{\partial v_i}{\partial x_j} \quad (19)
\end{aligned}$$

where the following definitions have been used :

$$R \equiv \frac{gL^3 \alpha_0 (\Delta T_A - \Delta T)}{\nu_0 \kappa_0} \quad (\text{Rayleigh number})$$

$$R_s \equiv \frac{gL^3 \gamma_0 (-\Delta c)}{\nu_0 D_0} \quad (\text{solute Rayleigh number})$$

$$Le \equiv \frac{D_0}{\kappa_0} \quad (\text{Lewis number})$$

$$Sc \equiv \frac{\nu_0}{D_0} \quad (\text{Schmidt number})$$

$$Gr \equiv \frac{\alpha}{\chi_0 C_{p0} \rho_0} \quad (\text{Grüneisen's constant})$$

$$S_T \equiv \frac{c_0(1 - c_0) D_0^* \gamma_0}{D_0 \alpha_0} \quad (\text{Soret separation number})$$

$$S_p \equiv \frac{\gamma_0^2 (1 - c_0)}{\rho_0 \mu_{1,1}^c \chi_0} \quad (\text{baro-diffusivity separation number}). \quad (20)$$

ε_1 , ε_2 and ε_3 are parameters defined by : $\varepsilon_1 = \alpha_0 |\Delta T|$, $\varepsilon_2 = \chi_0 |\Delta P|$ and $\varepsilon_3 = \gamma_0 |\Delta c|$. For the sake of simplicity the above equations may be compacted by using the following definitions :

$$MT_i \equiv \rho c (1 - c) D^* \frac{dT}{dx_i}$$

$$MP_i \equiv -D \gamma (1 - c) \frac{dP}{dx} \cdot \frac{1}{\mu_{1,1}^c}$$

$$Mc_i \equiv \rho D \frac{dc}{dx_i} \quad QT_i \equiv K \frac{dT}{dx_i}$$

$$QP_i \equiv -c(1 - c) \gamma TD^{**} \frac{dP}{dx_i} \quad (21)$$

and

$$Qc_i \equiv \rho c \mu_{1,1}^c TD^{**} \frac{dc}{dx_i}.$$

Table 2 show the values of the scale units and of the non-dimensional monomials that appear in equations (16)–(19). It is worth noting that $\partial(h_1 - h_2)/\partial x_i$ and A_2 have the same magnitude order as ε_1 , ε_2 or ε_3 .

6. APPROXIMATION EQUATIONS

The solution of equations (16)–(19) depends on parameter L and on the differences between boundaries $|\Delta T|$ and $|\Delta c|$. Since ε_1 , ε_2 and ε_3 are much lower than one, they are appropriate to develop a Taylor series expansion of the thermodynamic variables and the velocity in equations (16)–(19). As an additional advantage, the functional independence among ε_1 , ε_2 and ε_3 permits us to separate the dependences of the solutions with respect to $|\Delta T|$, L and $|\Delta c|$.

As an example of the procedure, the series expansion of the variable \tilde{T} is :

$$\begin{aligned}
\tilde{T} \equiv & \tilde{T}^{000} + \varepsilon_1 \tilde{T}^{100} + \varepsilon_2 \tilde{T}^{010} + \varepsilon_3 \tilde{T}^{001} + \varepsilon_1^2 \tilde{T}^{200} \\
& + \varepsilon_1 \varepsilon_2 \tilde{T}^{110} + \dots
\end{aligned}$$

Table 2. Values of the scale units and non-dimensional monomials (I.S.)

N_2/O_2 mixtures (I.S.)			
$T_0 \approx 300$	$P_0 \approx 10^5$	$c_0 \approx 0,76$	$\rho_0 \approx 1,2$
$\alpha_0 \approx 3,3 \times 10^{-3}$	$\chi_0 \approx 10^{-5}$	$\gamma_0 \approx -0,13$	$C_{p_0} \approx 10^3$
$\nu_0 \approx 1,5 \times 10^{-5}$	$\kappa_0 \approx 2 \times 10^{-5}$	$D_0 \approx 2 \times 10^{-5}$	$\alpha^* \approx -2 \times 10^{-2}$
$Pr \approx 0,7$	$Sc \approx 0,7$	$Le \approx 1$	$Gr \approx 0,3$
$S_T \approx 4 \times 10^{-4}$	$S_p \approx 3.10^{-3}$	$(1 - C_v/C_p) \approx 0,3$	
$NaCl$ aqueous solutions (I.S.)			
$T_0 \approx 300$	$P_0 \approx 10$	$c_0 \approx 0,94$	$\rho_0 \approx 1,041$
$\alpha_0 \approx 2 \times 10^{-4}$	$\chi_0 \approx 4 \times 10^{-10}$	$\gamma_0 \approx -0,7$	$C_{p_0} \approx 4 \times 10^3$
$\nu_0 \approx 10^{-6}$	$\kappa_0 \approx 1,4 \times 10^{-7}$	$D_0 \approx 1,5 \times 10^{-9}$	$\alpha^* \approx -0,8$
$Pr \approx 8$	$Sc \approx 7$	$Le \approx 10^{-2}$	$Gr \approx 0,1$
$S_T \approx 0,5$	$S_p \approx 1,3$	$(1 - C_v/C_p) \approx 6 \times 10^{-3}$	

As an other example, for the fluid material properties, the case of the diffusion coefficient is :

$$D' \equiv \frac{D}{D_0} = 1 + \frac{\varepsilon_1}{\alpha_0 D_0} \left(\frac{\partial D}{\partial T} \right)_0 ((T_s - T_0)' + A_1 \tilde{T}') + \frac{\varepsilon_2}{\chi_0 D_0} \left(\frac{\partial D}{\partial P} \right)_0 ((P_s - P_0)' + A_2 \tilde{P}') + \dots \quad (22)$$

It is worth noticing that the non-dimensional monomials such as $1/\alpha_0 D_0 (\partial D/\partial T)_0$, $1/\chi_0 D_0 (\partial D/\partial P)_0$, etc. which contain D derivatives of the order of unity, have been retained. In this way, the numerical values of the derivatives have been transferred to the monomials ε_1 , ε_2 and ε_3 and their products. This will allow us to numerically separate the different orders of magnitude in the original hierarchy of equations.

In zero order we have :

$$\frac{\partial V_i}{\partial x_i'} \equiv 0 \quad (23)$$

$$\sqrt{\frac{Sc}{Le} (R - Le R_s)} \left(\frac{\partial \tilde{c}^{000}}{\partial t} + \frac{\partial (c_s^{000} \delta_{3i} + A_3 c^{000})}{\partial x_i} v_i^{000} \right) = \frac{S_T A_1 \varepsilon_1}{\varepsilon_3} \frac{\partial^2 (\tilde{T}^{000})}{\partial x_i \partial x_i} + A_3 \frac{\partial^2 (\tilde{c}^{000})}{\partial x_i \partial x_i} \quad (24)$$

$$\frac{\partial V_i^{000}}{\partial t} + v_j^{000} \frac{\partial v_i^{000}}{\partial x_j} = - \frac{\partial \tilde{P}^{000}}{\partial x_i} + \sqrt{\frac{Pr}{R - Le R_s}} \left(\frac{\partial^2 v_i^{000}}{\partial x_j \partial x_j} \right) - \left(- \frac{A_1 \varepsilon_1}{A_2} \text{Sign}(\alpha) \tilde{T}^{000} + \frac{A_3 \varepsilon_3}{A_2} \text{Sign}(\gamma) \tilde{c}^{000} \right) \quad (25)$$

$$\sqrt{Pr(R - Le R_s)} \left(\frac{\partial \tilde{T}^{000}}{\partial t} + \frac{\partial (T_s^{000} \delta_{3i} + A_1 \tilde{T}^{000})}{\partial x_i} v_i^{000} \right) - \left(1 - \frac{C_{v0}}{C_{p0}} \right) \frac{\varepsilon_2}{\varepsilon_1} v_3^{000} \cdot \frac{dP_s^{000}}{dx_3} = A_1 \cdot \frac{\partial^2 \tilde{T}^{000}}{\partial x_i \partial x_i} + \frac{S_T Le \varepsilon_3}{S_p \varepsilon_1} \left(1 - \frac{C_{v0}}{C_{p0}} \right) A_3 \cdot \frac{\partial^2 \tilde{c}^{000}}{\partial x_i \partial x_i} \quad (26)$$

In what follows, we will analyze the conditions that must be fulfilled in order to get the numerical splitting of the different orders in the hierarchy of equations.

7. NUMERICAL SEPARATION OF THE DIFFERENT ORDERS IN THE EXPANSION

The three-parameter perturbative expansion developed in the last section permits us to obtain a hierarchy of equations containing the successive powers of the parameters ε_1 , ε_2 and ε_3 . Although the mathematical procedure seems to be correct, it is not always possible to avoid an overlapping of numerical values of the different orders in the obtained hierarchy. The aim of this section is to analyze the restrictions on the boundary conditions that are necessary in order to assure the numerical splitting of the n first orders in

the hierarchy (n being a previously chosen value). Obviously, if one limits the relative variability of the numerical values of the parameters ε_1 , ε_2 and ε_3 , it is possible to get the numerical separation of the different orders in the hierarchy. The following theorem imposes a limit to this variability :

Theorem I

Let us suppose that the three parameters verify the relationship: $\varepsilon_i \leq \varepsilon_j \leq \varepsilon_k \ll 1$. A necessary and sufficient condition for the successive natural powers of these parameters not to overlap, up to the order n , is that :

$$A^n > \varepsilon_k \geq A^{n+1} \quad (27)$$

being $A \equiv \varepsilon_i/\varepsilon_k$.

Proof

1. *Necessary condition.* If the numerical separation of the successive powers of the monomials, up to the order n , has been achieved one has :

$$1 \gg \varepsilon_k \geq \varepsilon_j \geq \varepsilon_i > \varepsilon_k^2 \geq \varepsilon_j^2 \geq \varepsilon_i^2 > \dots \geq \varepsilon_k^n \geq \varepsilon_j^n \geq \varepsilon_i^n > \varepsilon_k^{n+1} \geq \varepsilon_j^{n+1} \geq \varepsilon_i^{n+1} \leq \varepsilon_k^{n+2} \quad (28)$$

if one divides equation (28) by ε_k^n or ε_k^{n+1} one obtains respectively :

$$\frac{\varepsilon_i^n}{\varepsilon_k^n} (\equiv A^n) > \frac{\varepsilon_k^{n+1}}{\varepsilon_k^n} = \varepsilon_k \quad \text{or} \quad \dots \frac{\varepsilon_i^{n+1}}{\varepsilon_k^{n+1}} (\equiv A^{n+1}) \leq \varepsilon_k$$

and, finally, one achieves equation (27).

2. *Sufficient condition.* If one multiplies (27) by ε_k^n and ε_k^{n+1} , respectively one gets :

$$\varepsilon_i^n > \varepsilon_k^{n+1} \geq \frac{\varepsilon_i^{n+1}}{\varepsilon_k} \quad \text{and} \quad \varepsilon_i^n \cdot \varepsilon_k > \varepsilon_k^{n+2} \geq \varepsilon_i^{n+1}$$

from which the following inequality is reached :

$$\varepsilon_i^n > \varepsilon_k^{n+1} \geq \varepsilon_j^{n+1} \geq \varepsilon_i^{n+1} \leq \varepsilon_k^{n+2} \quad (29)$$

if one takes the n -root in equation (29), one gets :

$$\varepsilon_i > \varepsilon_k^{(n+1)/n} \geq \varepsilon_j^{(n+1)/n} \geq \varepsilon_i^{(n+1)/n}.$$

From this inequality, one has $\varepsilon_k \geq \varepsilon_j \geq \varepsilon_i$ and, also, $\varepsilon_i > \varepsilon_k^{(n+1)/n} > \varepsilon_k^2$ for $n > 2$. From equation (29) it is possible to take the successive powers of the inequality until $(n-1)$ th and so obtain the relationship of equation (28) by iteration.

This theorem gives rise to two corollaries that will be useful in getting the numerical splitting sought :

Corollary I

The inequality $A^n > \varepsilon_k \geq A^{n+1}$ is equivalent to :

$$\varepsilon_k^{(n+1)/n} < \varepsilon_i \leq \varepsilon_j \leq \varepsilon_k$$

Proof

If one takes the n th-root in equation (27), one has $\varepsilon_i/\varepsilon_k > \varepsilon_k^{(1/n)}$, and multiplying by ε_k one gets the required inequality.

Corollary II

The inequality $A^n > \varepsilon_k \geq A^{n+1}$ is equivalent to:

$$\varepsilon_i \leq \varepsilon_j \leq \varepsilon_k < \varepsilon_i^{(n-1)/n}$$

Proof

If one takes into account the relationship obtained in Corollary I, $\varepsilon_i/\varepsilon_k > \varepsilon_k^{(1/n)} \geq \varepsilon_j^{(1/n)} \geq \varepsilon_i^{(1/n)}$ and multiplies it by $\varepsilon_k/\varepsilon_i^{(1/n)}$ the corollary is demonstrated.

The application of these two corollaries to the present problem permits us to choose one of the parameters as a reference and to determine the variability range of the other two parameters with respect to it. The choosing of ε_2 as a reference has some advantages, because it is directly related to the layer thickness. It is also possible to choose the order for which the numerical splitting is assured (in most practical applications $n = 2$ is sufficient).

Let us analyze the two possibilities: (a) if ε_1 and ε_3 are greater than ε_2 , then Corollary II applies and $\varepsilon_2 \leq \varepsilon_j \leq \varepsilon_k < \varepsilon_2^{2-1/2}$; (b) if ε_2 were the greatest, then Corollary I would apply and $\varepsilon_2^{(2+1)/2} < \varepsilon_i \leq \varepsilon_j \leq \varepsilon_2$.[†] Consequently, the range of variability of these parameters and their binary products, which are compatible with the separation of powers up to the second order, is given around the values of ε_2 determined by:

$$1 > \varepsilon_2^{1/2} > \varepsilon_j > \varepsilon_2^{3/2} \quad (30)$$

where $j = 1, 3$. In order to be sure that the monomials are much lower than one, we can use $\varepsilon_2 < 0.01$ as a superior limit. In Fig. 1, region I corresponds to the monomials whose values are greater than $\varepsilon_2^{1/2}$ (for a given value of ε_2). These values belong numerically to the zero order in the hierarchy of equations (it has been assumed that the numerical splitting in the different orders has been obtained). Region II, whose values are limited by the inequality of equation (30), corresponds to monomials whose values are of the first order (f.i. ε_1 and ε_3). Region III, whose values are lower than $\varepsilon_2^{3/2}$ (for a given value of ε_2), corresponds to the monomials of the second or even superior order.

It is worth noticing that the inequality of equation (30) imposes certain restrictions on the temperature and pressure differences between boundaries, via parameters ε_1 and ε_2 , respectively. In the next section we will consider the consequences of these conditions on the zero-order monomials of the hierarchy of equations.

8. ZERO-ORDER MONOMIALS

For certain values of the layer thickness, some of the monomials retained in the zero-order (equations (23)–(26)) have numerical values lower than $\varepsilon_2^{1/2}$ and consequently, should be included in a superior order if we want to have a rigorous numerical splitting valid up to the second order. With this in mind, it is necessary to determine the values of the monomials that

multiply the terms which represent the Soret and the Dufour effects as well as the effect of the hydrostatic pressure gradient in the heat equation. In what follows, the numerical relevance in zero-order of these effects will be discussed in relation to the fluid layer thickness.

Soret effect. The monomial corresponding to the Soret is (see equation (34)):

$$S_T A_1 \varepsilon_1 / \varepsilon_3. \quad (31)$$

The Soret separation number, S_T , is much lower than one in the case of gas mixtures and slightly lower than one in the case of liquid solutions (see Table 2). In order to evaluate A_1 we can consider that the difference between ΔT and $\Delta \tilde{T}$ is produced by the adiabatic convective ascent of the hot fluid elements. This is due to the fact that the time of ascent through the layer is much lower than the thermal and the diffusive relaxation times. The adiabatic cooling of an ascent fluid element in a layer is given by $\Delta T_A = -g\alpha T_0 L / C_{p_0}$. This cooling is very noticeable in gas layers, from it, it is possible to make the following calculation:

$$\begin{aligned} A_1 &= (\tilde{\Delta T} - \Delta T) / \Delta T = 1 + g\alpha T_0 L / (\Delta T \cdot C_{p_0}) \\ &= 1 + \left(1 - \frac{C_v}{C_p}\right) \frac{\varepsilon_2}{\varepsilon_1}. \end{aligned} \quad (32)$$

If one takes into account equation (31), the expression of the monomial is:

$$S_T A_1 \varepsilon_1 / \varepsilon_3 = S_T \varepsilon_1 / \varepsilon_3 + S_T \left(1 - \frac{C_v}{C_p}\right) \frac{\varepsilon_2}{\varepsilon_3}. \quad (33)$$

Figures 2(a)–(b) represent, in logarithmic scale, the domain of variation for the monomial values (the surface between the continuous straight lines is marked with ■) as a function of ε_2 , for layers of dry air (for details see Table 2) and of salt water, respectively. It must be noted that whereas quotient $\varepsilon_2/\varepsilon_3$ varies in the range $\varepsilon_2^{-1/2} \geq \varepsilon_2/\varepsilon_3 \geq \varepsilon_2^{1/2}$, the quotient $\varepsilon_1/\varepsilon_3$ varies in a wider range $\varepsilon_2^{-1} \geq \varepsilon_1/\varepsilon_3 \geq \varepsilon_2^1$. As a rule, the second term of these monomials is relevant in the case of gases, but not in the case of liquids. The three regions of Fig. 1 have been superimposed in Fig. 2(a)–(b) as references in order to determine the order of the hierarchy of equations to which these monomials belong. The same procedure will be used in the remaining figures.

In the case of the gas mixture, it should be noticed that the Soret effect is numerically of a more superior order than the first, for values of $\log(\varepsilon_2)$ greater than -1.3 (or $L > 400$ m), but may be of a zero-order, for values of $\log(\varepsilon_2)$ lower than -2.2 (or $L < 55$ m). In this case there is a dependence on the relation between the temperature and concentration gradients. In the case of salt water, the analogous lower and upper limits of $\log(\varepsilon_2)$ are -0.2 (or $L > 130\,000$ m) and -0.4 (or $L < 85\,000$ m), respectively. In both cases the limits exceed what is physically reasonable and mathematically convenient and, as a consequence, the

[†] The case in which ε_2 lies between ε_1 and ε_3 is trivial.

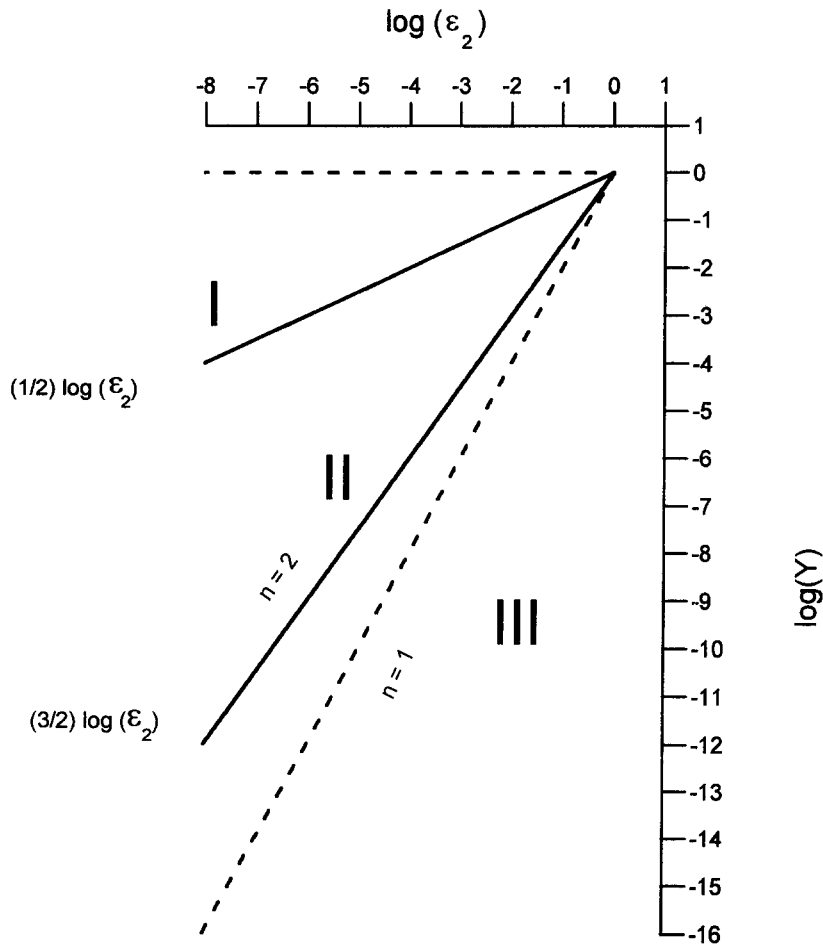


Fig. 1. Domain of validity for the parameters ε_1 and ε_3 with respect to ε_2 (continuous lines correspond to $n = 2$ and discontinuous lines correspond to $n = 1$). Region I corresponds to zero-order, region II to first order and region III to superior orders.

Soret effect is relevant in all kinds of layers, within a wide range of thicknesses.

Dufour effect. The term corresponding to the Dufour effect appears in equation (26) multiplied by the monomial:

$$(S_T L e / S_P) \left(1 - \frac{C_v}{C_p} \right) (\varepsilon_3 / \varepsilon_1). \quad (34)$$

This monomial is lower than one in the case of gas mixtures, but much lower than one for liquid solutions (see Table 2). The quotient $\varepsilon_3 / \varepsilon_1$ varies in the interval $\varepsilon_2^{-1} \geq \varepsilon_3 / \varepsilon_1 \geq \varepsilon_2^1$. Figure 2(a)–(b) represents (in logarithmic scale) the domain of variation for the monomial values (surface between the continuous straight lines marked with ●) as a function of ε_2 for dry air and for salt water layers, respectively. In the case of the gas mixture, the Dufour effect has an order of magnitude greater than the first, for $\log(\varepsilon_2)$ values greater than -0.5 ($L > 2800$ m), whereas it may be of zero-order for $\log(\varepsilon_2)$ values lower than -1 ($L < 880$ m), depending on the relationship between the gradients. In the case of salt water, both superior and inferior limits are greater than one, which con-

firms that the Dufour effect is relevant in all kinds of layers, within a wide range of physically reasonable thicknesses.

Influence of the hydrostatic field. The numerical influence of the hydrostatic pressure field on the heat equation is given by the monomial:

$$\left(1 - \frac{C_v}{C_p} \right) \frac{\varepsilon_2}{\varepsilon_1}. \quad (35)$$

Figure 3(a) shows, in logarithmic scale, the domain of variation for the monomial values (the surface between the continuous straight lines marked with +) as a function of ε_2 for dry air layers. Figure 3(b) refers to salt water. In the case of the gas mixture, the H.F. influence is numerically of an order greater than the first, for $\log(\varepsilon_2)$ values greater than -0.3 ($L > 4400$ m), whereas it may be of zero-order for $\log(\varepsilon_2)$ values lower than -0.5 ($L < 2800$ m), depending on the relation between gradients. In the case of the salt water, the analogous lowest and highest limits of $\log(\varepsilon_2)$ are -1.1 ($L > 17000$ m) and -2.2 ($L < 1300$ m), respectively.

Variability of monomial $(R - Le R_s)^{1/2}$. The value

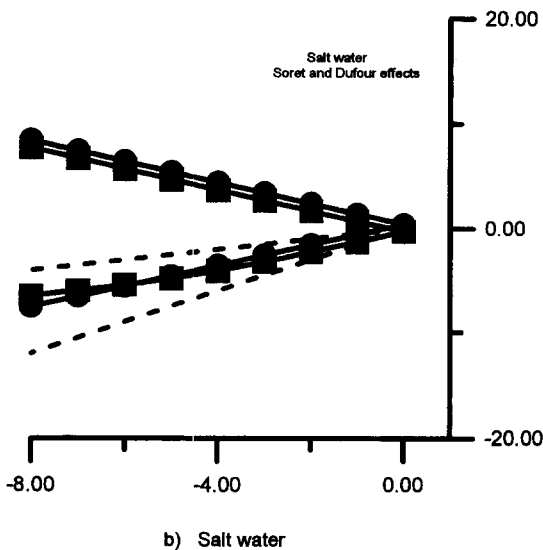
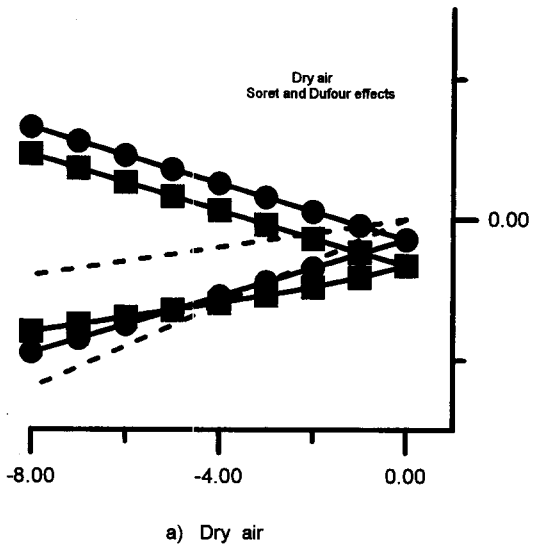


Fig. 2. (a) Domains of validity (surface between continuous lines) for the Soret effect (■) and Dufour effect (●) in dry air; (b) domains of validity (surface between continuous lines) for the Soret effect (■) and Dufour effect (●) in salt water.

of the monomial $(R - Le R_s)^{1/2}$ depends implicitly on parameters ε_1 , ε_2 and ε_3 through the differences between boundaries ΔT , Δc and $\rho g L$. For this reason, the domain of possible values for this monomial depends on the permitted values of ε_2 . This monomial appears in equations (24) and (26), multiplied by factors of magnitudes very close to one and its inverse value appears in equation (25) multiplied by a factor that is also of the order of magnitude of one. The domains of permitted values for the monomials (continuous lines marked with \times) and their inverse values (continuous lines marked with Δ) are shown in Fig. 3(a) which corresponds to dry air and Fig. 3(b) which corresponds to salt water. $(R - Le R_s)^{1/2}$ and its inverse

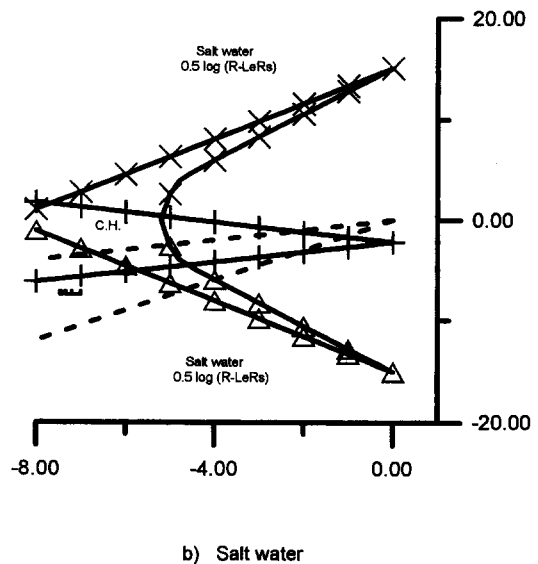
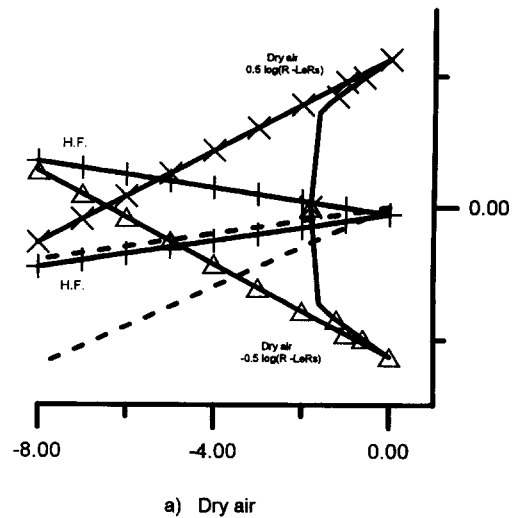


Fig. 3. (a) Domains of validity (surface between continuous lines) for the H.F. (+) contribution, for the monomial $(R - Le R_s)^{1/2}$ (\times) and for its inverse (Δ) in dry air; (b) domains of validity (surface between continuous lines) for the H.F. (+) contribution, for the monomial $(R - Le R_s)^{1/2}$ (\times) and for its inverse (Δ) in salt water.

value impose some restrictions on the domains of validity of the zero-order equations (23)–(26).

The above discussion permits us to delimit the range of validity of each of the terms studied. The analysis may be considered a numerical estimation of these terms, as related to the parameter ε_2 and its powers. These ideas may be, obviously, generalized by means of the following lemma.

Lemma

Let us assume that the non-dimensionalized monomial M belongs to one of the non-dimensionalized equations of the hierarchy. The order in which this term must be included within the hierarchy of equa-

tions in order to separate it numerically, may be determined by looking for a natural number m that verifies the following inequality :

$$\varepsilon_2^{(n-1)/n} > \frac{\mathbb{M}}{\varepsilon_2^m} > \varepsilon_2^{(n+1)/n} \quad (36)$$

m being the order of the hierarchy at which \mathbb{M} belongs and n the maximum order of the perturbative expansion for which the numerical split of the terms belonging to the different order in the hierarchy is obtained.

9. CONCLUSIONS

(1) A method has been proposed that permits us to study the behavior of convective fluid layers. The system may be numerically split in a hierarchy of equations by means of a three parameter perturbative expansion, which is related to the boundary conditions of the layer. Although the paper considers only the simple case of two-component mixtures, the procedure may be easily generalized to multi-component systems. In this case it is necessary to use additional parameters (similar to ε_3), representing the difference of the various mass fractions between the boundaries.

(2) The method may be generalized to any other problem whose solution is obtained from a system of equations that may be non-dimensionalized. The procedure permits us to state, in a rigorous way, what the numerical importance is of each of the terms appearing in the hierarchy of equations.

(3) The first orders of the hierarchy of equations describing the behavior of convective fluid layers have been studied. The layer thickness has been calculated in such a way that the terms corresponding to the Soret and the Dufour effects, or the term corresponding to the influence of the hydrostatic field on the heat equation, are retained. It must not be forgotten that, in the case of impervious walls, the thermal diffusion relates to the temperature and concentration differences between the layer boundaries. This relationship imposes a restrictive link to the relative variations of ε_1 and ε_3 .

REFERENCES

1. Boussinesq, J., *Theorie Annalytique de la Chaleur*, Vol. 1. Gauthier-Villars, Paris, 1903, pp. 154–176.
2. Spiegel, E. A. and Vernois, G., On the Boussinesq approximation for compressible fluids. *Astrophysical Journal*, 1960, **131**, 442–447.
3. Mihaljan, J. M., A rigorous exposition of the Boussinesq approximation applicable to a thin layer of fluid. *Astrophysical Journal*, 1962, **136**, 1126–1133.
4. Malkus, W. V. M., Summer study program in geophysical fluid dynamics of the woods hole oceanographic institution, U.S. National Technical Information, PB-186314, Vol. 1, 1964, pp. 1–12.
5. Pérez-Cordón, R. and Velarde, M. G., On the (non-linear) foundations of the Boussinesq approximation applicable to a thin layer of fluid. *Journal de Physique*, 1975, **36**, 591–601.
6. Verlarde, M. G. and Pérez-Cordón, R., On the (non-linear) foundations of the Boussinesq approximation applicable to a thin layer of fluid : II. Viscous dissipation and large cell gap effects. *Journal de Physique*, 1976, **37**, 177–182.
7. Gray, D. D. and Giorgini, A., The validity of the Boussinesq approximation for liquids and gases. *International Journal of Heat & Mass Transfer*, 1976, **19**, 545–551.
8. de Boer, P. T. C., Thermally driven motion of strongly heated fluids. *International Heat & Mass Transfer*, 1984, **27**, 2239–2251.
9. de Boer, P. T. C., Thermally driven motion of highly viscous fluids. Fluid Dynamics and Aerodynamics Program, report FDA-85-2, Ithaca, 1985.
10. Fröhlich, J. and Laure, P., Marginal stability in the Rayleigh–Benard problem with large departures from Boussinesq approximation. *European Journal of Mechanics B*, 1991, **10**, 329–329.
11. Bennacer, R., Sun, L. Y., Toguyeni, Y., Gobin, D. and Benard, C., Structure d'écoulement et transfert de chaleur par convection naturelle au voisinage du maximum de densité. *International Journal Heat & Mass Transfer*, 1993, **36**, 3329–3342.
12. Koschmieder, E. L., The wavelength of supercritical surface tension driven Benard Convection. *European Journal of Mechanics B*, 1991, **10**, 233–237.
13. Bodenschatz, E., Cannell, D. S., de Bruyn, Jr. R., Ecke, R., Hu, Y. C., Lerman, K. and Ahlers, G., Experiments on three systems with nonvariational aspects. *Physica D*, 1992, **61**, 77–93.
14. Xi, H. W., Gunton, J. D., and Viñals, J., Sprial-pattern formation in Rayleigh–Benard convection. *Physics Review E*, 1993, **47**, 2987–2990.
15. Bergean, A., Henry, D. and Benhadid, H., Marangoni–Benard instability in microgravity conditions with Soret effect. *International Journal Heat & Mass Transfer*, 1994, **37**, 1545–1562.
16. Velarde, M. G. and Schechter, R. S., Thermal diffusion and convective stability. II. An analysis of the convected fluxes. *Physics of Fluids*, 1972, **15**, 1707–1714.
17. McDougall, T. J., Double diffusive convection by coupled molecular diffusion. *Journal of Fluid Mechanics*, 1983, **126**, 379–397.
18. Linz, S. J., Lücke, M., Müller, H. W. and Niederländer, Convection in binary fluid mixtures: Traveling waves and lateral currents. *Physics Review A*, 1988, **38**, 5727–5741.
19. Srinivasan, J. and Angirasa, D., Numerical study of double-diffusive free convection from a vertical surface. *International Journal of Heat & Mass Transfer*, 1988, **31**, 2033–2038.
20. Srinivasan, J. and Angirasa, D., Laminar axisymmetric multicomponent buoyant plumes in thermally stratified medium. *International Journal of Heat & Mass Transfer*, 1990, **33**, 1751–1757.
21. Stein, N. D., Exact sine series solution for oscillatory convection in binary fluid. *Physics Review A*, 1991, **43**, 786–773.
22. Hort, W., Linz, S. J. and Lücke, M., Onset of convection in binary gas mixture: role of Dufour effect. *Physics Review A*, 1992, **45**, 3737–3748.
23. Zimmermann, G., Müller, U. and Davis, S. H., Benard convection in binary mixtures with Soret effects and solidification. *Journal of Fluid Mechanics*, 1992, **238**, 657–682.
24. Jeffreys, H., The instability of a compressible fluid heated below. *Proceedings of Cambridge Philosophical Society*, 1930, pp. 170–172.
25. Pérez-Cordón, R., and Aguilar-Peris, J., Contribución al análisis de los campos hidrostáticos en capas de fluidos multicomponentes. *Revista de la Real Academia Ciencias*, 1987, **81**, 315–337.
26. Pérez-Cordón, R., and Aguilar-Peris, J., Campos hidrostáticos de fluidos multicomponentes en capas líquidas y gaseosas. *Anales de Física*, 1986, **82**, 250–264.